

# On the relation between zenith sky brightness and horizontal illuminance

M. Kocifaj,<sup>1,2★</sup> Th. Posch<sup>3</sup> and H. A. Solano Lamphar<sup>4,5</sup>

<sup>1</sup>*Department of Experimental Physics, Faculty of Mathematics, Physics and Informatics, Comenius University, Mlynská dolina, 842 48 Bratislava, Slovak Republic*

<sup>2</sup>*ICA, Slovak Academy of Sciences, Dúbravská cesta 9, 845 03 Bratislava, Slovak Republic*

<sup>3</sup>*Universität Wien, Institut für Astrophysik, Türkenschanzstrasse 17, A-1180 Wien, Austria*

<sup>4</sup>*Instituto de Investigaciones Lumínicas, Los Mochis, Sinaloa, Mexico*

<sup>5</sup>*Cátedras CONACYT, Instituto de investigaciones Dr José María Luis Mora, Programa Interdisciplinario de Estudios Metropolitanos, Plaza Valentín Gómez Farías #12 Col. San Juan Mixcoac México D.F. C.P 03730*

Accepted 2014 October 24. Received 2014 October 23; in original form 2014 September 1

## ABSTRACT

The effects of artificial light at night are an emergent research topic for astronomers, physicists, engineers and biologists around the world. This leads to a need for measurements of the night sky brightness (= diffuse luminance of the night sky) and nocturnal illuminance. Currently, the most sensitive light meters measure the zenith sky brightness in  $\text{mag}_V/\text{arcsec}^2$  or – less frequently – in  $\text{cd m}^{-2}$ . However, the horizontal illuminance resulting only from the night sky is an important source of information that is difficult to obtain with common instruments. Here we present a set of approximations to convert the zenith luminance into horizontal illuminance. Three different approximations are presented for three idealized atmospheric conditions: homogeneous sky brightness, an isotropically scattering atmosphere and a turbid atmosphere. We also apply the resulting conversion formulae to experimental data on night sky luminance, obtained during the past three years.

**Key words:** scattering – atmospheric effects – light pollution – methods: numerical.

## 1 INTRODUCTION

Artificial light emissions at night have become a worldwide environmental problem that is constantly growing in most countries due to land consumption, the rising populations of many big cities, industrialization and the increasing luminous efficacy of modern light sources (Cinzano 2000b; Cinzano, Falchi & Eldvidge 2001; Kyba et al. 2013; Bennie et al. 2014). The need for a continuous quantification of the problem is increasing in various disciplines (astronomy, environmental sciences, sleep research, entomology and many others). For this purpose, many different devices, such as the sky quality meter (SQM: Cinzano 2005), charge-coupled device sensor (CCD: Falchi 1999, 2011; Cinzano & Falchi 2003; Duriscoe, Luginbuhl & Moore 2007), digital single-lens reflex camera (DSLR: Solano Lamphar & Kunderlik 2014) or other light meters, are available or in development. These devices have opened the field of long-term studies and statistical analysis of light pollution and have enabled researchers to obtain a large amount of data from all over the world (Riddle et al. 2008; Biggs et al. 2012; Pun & So 2012; Puschnig, Posch & Uttenthaler 2014). The SQM is one of the most widely used instruments to measure night sky brightness in many countries. This device is a compact photometer with a portable design that allows the night sky brightness to be quanti-

fied easily and continuously (Cinzano 2005). Due to its availability, the SQM has commonly been used by amateur astronomers in the search for suitable dark sky places. Furthermore, it has also been used in various serious research works (Kolláth 2010; Falchi 2011; Kyba et al. 2011; Puschnig et al. 2014).

Experimental characterization of the artificial night sky brightness has received considerable attention at astronomical observatories (Garstang 1989b, 1991; Aubé & Kocifaj 2012; Guo et al. 2014), since it reduces the contrast between the sky and celestial objects. In professional and amateur astronomy, the sky brightness is usually measured as zenith sky brightness in the  $V$  band, with units of  $\text{mag}_V/\text{arcsec}^2$ . In other fields, such as the lighting engineering community, the luminance in  $\text{cd m}^{-2}$  is more commonly used. Measurements expressed in  $\text{mag}_V/\text{arcsec}^2$  can be converted to  $\text{cd m}^{-2}$  under some assumptions regarding the spectra of the light source(s). A more complex task, on which we focus here, is to obtain the horizontal illuminance from zenith sky brightness data.

During the past years, the zenith sky brightness has been measured proficiently and thus a great amount of data from different regions and periods of time became available. However, it is known that the horizontal illuminance is the most representative source of information about the total amount of light that reaches a given surface. Of course, other quantities such as the vertical illuminance, average sky brightness and maximum sky brightness are also in use. So far, there is a lack of data regarding illuminance recorded in near-natural nocturnal landscapes. The amount of nocturnal

★E-mail: kocifaj@savba.sk

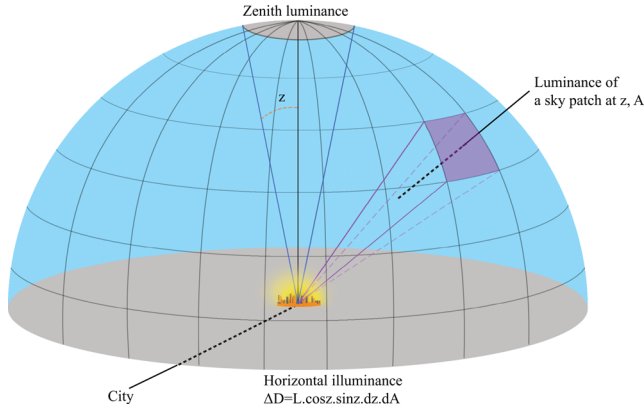


**Figure 1.** The horizontal illuminance is an integral of the cosine projected sky brightness. The sky brightness is integrated over all sky patches with zenith angles  $z \in [0, \pi/2]$  and azimuth angles  $A \in [0, 2\pi]$ .

radiation recorded at the ground is required not only by astronomers and engineers but also by biologists and environmentalists, who investigate the ecological consequences of artificial night lighting expressed in terms of illuminance values (Rich & Longcore 2005; Wise 2007; Perry et al. 2008; Geffen et al. 2014). As explained in the book by Rich & Longcore (2005), illuminance values may be extremely low in nocturnal environments (see e.g. table 1.1 and fig. 2.2 in their book), with variations depending on solar and lunar altitudes. A typical illuminance value for a clear moonless night with the stars and the natural airglow as the only light sources is of the order of 0.001 lux and it has been suggested that the circadian rhythm of different bat species can be affected by illuminance levels as low as  $10^{-5}$  lux (Rich & Longcore 2005). However, since most illuminance meters have been designed for daylight measurements, the absence of sensitive devices is an important constraint. Therefore, there is a real need for the conversion of zenith sky brightness into horizontal illuminance based on the principles of radiative transfer.

In this article, we present approximation methods for the conversion of the more readily available zenith luminance into horizontal luminance, assuming that the angular distribution of the night sky brightness follows certain laws and that the diffuse luminance is considered as the dominant source of horizontal illuminance in a specific place (see Fig. 1).

To summarize again, the motivation of our study is related to the following circumstances.

(i) Illuminance measurements are difficult to perform in the field. One of the reasons is that in real environments there could be a significant masking of the horizon. The orographic conditions or high objects (such as trees, buildings and monuments, among others) block the horizontal light, making it impossible to determine the horizontal illuminance precisely, including the radiation from low elevation angles.

(ii) There is a lack of sensitive illuminance detectors. Devices that can measure nocturnal horizontal illuminance in the millilux range are expensive and not widely available (an exception is the light meter described by Müller, Wuchterl & Sarazin 2011). Therefore, most measurements of natural nocturnal illuminance values are extremely difficult to perform with the usual instruments.

(iii) Information on the nocturnal horizontal illuminance is crucial for many research topics, including the emerging field of ecological consequences of light at night.

As a core part of this article, three different approximations corresponding to three atmospheric conditions are developed. Homogeneous sky brightness is considered as the first case. The second case is an isotropically scattering atmosphere; a turbid atmosphere is considered as the third case.

## 2 CONVERTING ZENITH SKY BRIGHTNESS INTO HORIZONTAL ILLUMINANCE

The distribution of the night sky brightness depends on the physical state of the atmospheric environment, including turbidity, aerosol optics and cloud physics, but also other factors such as the position of the observer with respect to the dominant light sources, cloud altitude, upward emission as a function of the zenith angle and potential masking of the horizon by obstacles and the surrounding terrain. Strictly speaking, the conversion of zenith brightness to horizontal illuminance is only possible if a mapping function has a theoretical foundation and can be parametrized using the individual, time-dependent physical characteristics of the local night sky.

However, idealized cases can be considered for which a straightforward, 'global' relation between zenith sky luminance and horizontal illuminance exists. This is the topic of the next subsections.

### 2.1 Homogeneous sky brightness

The first idealized situation for which we shall now calculate the conversion factor between zenith luminance and horizontal illuminance is the case of homogeneous sky brightness and the visibility of a full hemisphere down to the mathematical horizon. Let  $\phi$  be the azimuth angle,  $z$  the zenith angle and  $B(\phi, z)$  the background sky brightness (luminance) in  $\text{cd m}^{-2}$ . Then the present approximation can be written as the simple condition

$$B(\phi, z) = \text{const.} = B_0 \quad \forall \phi \in (0, 2\pi), \forall z \in (0, \pi/2). \quad (1)$$

The horizontal (*diffuse*) illuminance  $D$  in lux then becomes

$$D = \int_{\phi=0}^{\phi=2\pi} \int_{z=0}^{z=\pi/2} B(\phi, z) \sin z \cos z \, d\phi \, dz. \quad (2)$$

Under the above condition (constant  $B(\phi, z)$ ), this expression is equivalent to

$$D = B_0 \int_{\phi=0}^{\phi=2\pi} d\phi \int_{z=0}^{z=\pi/2} \sin z \cos z \, dz. \quad (3)$$

Using the substitution method, it can be shown that this integral yields

$$D = 2\pi B_0 \times \frac{1}{2} = \pi B_0, \quad (4)$$

so the conversion factor equals  $\pi$  in this case.

We assume that the naturally dark, unpolluted night sky, with no scattering of moonlight and only low airglow activity, has a luminance of  $2 \times 10^{-4} \text{ cd m}^{-2}$  (Luginbuhl, Boley & Davis 2014). Such a luminance, if it is evenly distributed over the full hemisphere, will produce a horizontal illuminance of 0.63 mlux (in the absence of any deviations from the mathematical horizon). In a desert with no light pollution and very low horizon, this value may be considered as an approximation of the natural nocturnal horizontal illuminance during new moon nights. Note that Cinzano and Falchi (2012) expect a slightly higher natural nocturnal illuminance of 0.8 mlux (which is due to the fact that natural skies – even without any light pollution – tend to be brighter close to the horizon than at the zenith).

Based on equation (2), the horizontal illuminance can also be derived for the general case of non-homogeneous sky brightness. If the actual sky brightness  $B(\phi, z)$  at a given location and time is known, e.g. from a calibrated all-sky-camera image, the quantity  $D$  can be derived individually (and it will be time-dependent as  $B(\phi, z)$ ). Nevertheless, we shall derive other idealized conversion factors between  $B_0$  and  $D$  in this article, since the full spatially resolved information on  $B(\phi, z)$  is often not available.

## 2.2 Two-stream approximation for uniformly emitting surface

Nowadays, excessive lighting is not only an agenda of large metropolitan regions, but can be also related to diffusely populated areas. If the ground-based light emissions can be simulated as a continuum, the rapid decay of sky glow from distant sources will be efficiently counterbalanced by their growth in number (Cinzano 2000a). A modelling of light emissions from large territories is extremely difficult – or rather impossible – when the detailed topology of the light sources with their physical, geometrical and spectral heterogeneities is taken into account. To overcome these difficulties, an averaging over a statistically large set of light sources can be implemented in the form of a uniformly emitting surface. This allows for a simplified solution of the radiative transfer equation in a plane-parallel atmosphere. In the traditional two-stream concept, the upward and downward radiative fluxes are used, while Garstang (1989a) introduced a fraction  $F$  of the light that is emitted directly into the upper hemisphere at angles above the horizontal. The complementary fraction  $(1 - F)$  directed downwards undergoes reflection by the underlying surface. An approximate formula for the radiant intensity pattern of a Lambertian emitting surface was derived by Garstang (1989a) and is given as

$$I_{\text{up}}(z) = \frac{LP}{2\pi} [2G(1 - F) \cos z + 0.554Fz^4], \quad (5)$$

where  $LP$  is the total light output (typically measured in lumens or alternative units) and  $z$  is the zenith angle. Integrating equation (5) over the whole sky vault gives the total emission upwards:

$$\int_{4\pi} I_{\text{up}}(z) d\Omega = LP [G(1 - F) + F]. \quad (6)$$

The simplest approximation to atmospheric optics employs the Lambertian model with no attenuation, where the radiation directed downwards is somehow proportional to the amount of total emission upwards. In such a case, the ratio  $R$  of the horizontal illuminance  $D$  to zenith brightness  $B(z = 0)$  reads

$$R = \frac{D}{B(0)} \approx \frac{\int_{4\pi} I_{\text{up}}(z) d\Omega}{I_{\text{up}}(0)} = \pi \left[ 1 + \frac{F}{G(1 - F)} \right]. \quad (7)$$

If all luminous energy propagated upwards is only due to reflection from the ground (i.e.  $F = 0$ ), the ratio  $R$  would be exactly equal to  $\pi$ . This is the most routinely used factor relating the zenith brightness to the horizontal illuminance and it corresponds to what we have derived in the previous section for homogeneous sky brightness. However,  $R$  grows beyond all bounds for totally black surfaces (i.e.  $G = 0$ ), thanks to the two-lobed form of Garstang's function. If  $G = 0$ , the light propagates preferentially to low elevation angles, while the upward emission is completely missing (see fig. 1 in Kocifaj & Solano Lamphar 2014). In this model, the large values of  $R$  indicate that zenith brightness approaches extremely low values even if  $D > 0$ . The model with  $F = 0.15$  and  $G = 0.15$  is identical to what Garstang used and results in  $R \approx 2.2\pi$  (see Table 1). A further increase of the Earth's albedo, e.g. by snow,

**Table 1.** The approximate ratio  $R$  of horizontal illuminance to zenith brightness for the model of a uniformly emitting surface.  $F$  and  $G$  are Garstang's parameters, as defined in equation (5).

Model	$F$	$G$	$R$
no uplight	0	any	$\pi$
no reflected light	any	0	$\infty$
Garstang's model	0.15	0.15	$\pi/0.46$
dirty snow cover	0.15	0.45	$\pi/0.72$
snow cover (model 1)	0.15	0.55	$\pi/0.76$
snow cover (model 2)	0.15	0.65	$\pi/0.79$
snow cover (model 3)	0.15	0.75	$\pi/0.81$

is characterized by a monotonic decrease of  $R$  that asymptotically approaches the value  $\pi(1 - F)^{-1} = \pi/0.85$  for  $F=0.15$  and mirror-like surfaces. Basically, elevated reflectance translates to low ratios of  $D/B(0)$ , because the emissions to large zenith angles are reduced due to the cosine factor (see the first term on the right-hand side of equation 5). As a result, the contribution of the near-zenith region to the total downward radiative flux is affected only slightly.

## 2.3 Homogeneous attenuating atmosphere illuminated by a finite-sized light source

The solution introduced in the previous section poses a very strong requirement on light-source deployment. The problem of light propagation through the atmosphere is solved subject to the boundary condition assuming a surface emitting uniformly over a statistically large area. However, this is a largely idealistic scenario, since light sources are scarcely of this size. In reality, finite-sized sources need to be taken into account.

Under such conditions, the theoretical clear sky brightness in the first scattering approximation can be written in the form (Kocifaj 2007)

$$B(z) = \frac{A_0 S_0}{4\pi \cos z} \int_{h=0}^{\infty} I_{\text{up}}(z') \cos^2 z' \frac{k_{\text{sca}}(h)}{h^2} \times \exp \{ -(M' + M)\tau(h) \} P(\theta) dh, \quad (8)$$

where the total power  $S_0$  is emitted by a light source with area  $A_0$  to all directions  $z'(h)$ , where  $h$  is the altitude. For the sake of brevity, the azimuthal dependence is not indicated here and also shortened forms for the optical air masses  $M'$  and  $M$  at zenith distances  $z'$  and  $z$ , respectively, have been used. It has to be stated that an inverse cosine law can be used as an approximation to the optical air mass when zenith angles are below  $80^\circ$ . For non-conservative scattering, the atmospheric optical thickness reads

$$\tau(h) = \int_{H=0}^h \frac{k_{\text{sca}}(H)}{\tilde{\omega}} dH, \quad (9)$$

with  $k_{\text{sca}}$  being the atmospheric volume scattering coefficient. The parameters  $\tilde{\omega}$  and  $P(\theta)$  are the single scattering albedo and scattering phase function, both averaged over a corresponding atmospheric layer.

In a far-field approximation, equation (8) reduces to

$$B(z) \propto \frac{P(\pi)}{8\pi} I_{\text{up}}(z), \quad (10)$$

where light signals from nearly backscatter directions ( $\theta \approx \pi$ ) are assumed to be recorded at the ground. Since the horizontal illuminance is the cosine-projected brightness integrated over the whole

**Table 2.** The same as in Table 1, but for the model of a homogeneously attenuating atmosphere illuminated by a finite-sized light source.

Model	$F$	$G$	$R$
no uplight	0	any	$\pi/1.5$
no reflected light	any	0	$\infty$
Garstang's model	0.15	0.15	$\pi/1.06$
dirty snow cover	0.15	0.45	$\pi/1.32$
snow cover (model 1)	0.15	0.55	$\pi/1.35$
snow cover (model 2)	0.15	0.65	$\pi/1.37$
snow cover (model 3)	0.15	0.75	$\pi/1.39$

upper hemisphere:

$$D = 2\pi \int_{z=0}^{\pi/2} B(z) \cos z \sin z \, dz = \frac{P(\pi)}{6} G(1-F) + \frac{P(\pi)}{32} 0.554F \left( \frac{\pi^4}{8} - \frac{3\pi^2}{2} + 6 \right), \quad (11)$$

the ratio  $R$  is then

$$R = \frac{D}{B(0)} = \frac{2\pi}{3} \left[ 1 + \frac{0.35 F}{G(1-F)} \right]. \quad (12)$$

The atmospheric attenuation is especially important for light beams propagating along inclined trajectories, thus the zenith brightness is lowered less efficiently than signals from other elevation angles. As a result, the ratio  $R$  of horizontal illuminance to zenith brightness obtained from equation (7) is larger than that determined from equation (12): compare Table 1 with Table 2. The homogeneous atmosphere we have analysed here could be applicable to a boundary-layer atmosphere, where turbulence lifts the aerosol particles, actively resulting in efficient turbulent mixing. The restriction on single value  $P(\pi)$  is more acceptable under elevated turbidity conditions, where multiple scattering dominates, so the scattered signals have non-preferred directions. As a consequence, the scattering pattern asymptotically approaches that for isotropic scattering. However, the phase function is also largely smoothed in a non-polluted atmosphere, because the Rayleigh law dictates that  $P(\theta)$  is proportional to  $(1 + \cos^2\theta)$ .

#### 2.4 Analytical extension to an exponentially stratified atmosphere

Rather than forming a homogeneous layer, the Earth's atmosphere is vertically stratified. It is a common concept in radiative transfer theories to adopt an exponential model for the vertical profile of atmospheric constituents, such as aerosols or air molecules (McCartney 1977). Introducing the scaleheight  $h_{SC}$ , the atmospheric optical thickness  $\tau$ , as well as the volume scattering coefficient  $k_{sca}$ , can be expressed as follows:

$$\tau(h) = \tau_0 \exp\{-h/h_{SC}\}, \quad (13)$$

$$k_{sca}(h) = k_0 \exp\{-h/h_{SC}\}.$$

These simple formulae also allow for an analytical solution of equation (8):

$$B(z) \propto \frac{P(\pi)}{8\pi} I_{up}(z) (1 - \exp\{-2M\tau_0\}), \quad (14)$$

which extends equation (10) and makes it parametrizable through the atmospheric optical depth  $\tau_0$ . Note that equation (14) transforms to equation (10) if  $\tau_0$  approaches infinity or is large enough. This

is consistent with the conclusions to the previous section. On the other hand, the sky light is significantly suppressed or completely removed if  $\tau_0$  is as small as zero. A value of  $\tau_0 = 0$  represents an atmosphere-free environment, where neither attenuation nor scattering would occur. In the latter case, all the light emitted upwards is never scattered downwards, thus the luminance veil will be absent and the sky appears dark except for the stars and other extraterrestrial objects.

Because of the exponential term on the right-hand side of equation (14), no exact analytical solution to diffuse illuminance exists. However, we have found

$$D = \frac{P(\pi)}{6} \{G(1-F)[1 - \eta(\tau_0)] + F[0.35 - \rho(\tau_0)]\}, \quad (15)$$

where

$$\eta(x) = e^{-2x} [2x^2 - x + 1 - 4x^3 e^{2x} E_1(2x)] \quad (16)$$

is an exact solution and

$$\rho(x) = \frac{(0.2 + 1.2e^{-2x})}{4} e^{-x(2.8+3.3e^{-4x})} \quad (17)$$

is a fairly accurate approximation. The exponential integral  $E_1$  for values  $x < 1$  can be written as

$$E_1(x) = -\ln(x) - \gamma + x - \frac{1}{4}x^2 + \frac{1}{18}x^3 - \dots, \quad (18)$$

where  $\gamma = 0.577\dots$  is the Euler constant. The ratio of horizontal illuminance to zenith brightness is then

$$R = \frac{4\pi G(1-F)[1 - \eta(\tau_0)] + F[0.35 - \rho(\tau_0)]}{6 G(1-F)(1 - e^{-2\tau_0})}. \quad (19)$$

If the light emissions upwards are due only to reflected light, the above formula reads

$$R_{\text{no uplight}} = \frac{4\pi}{6} \frac{1 - \eta(\tau_0)}{1 - e^{-2\tau_0}}, \quad (20)$$

while exclusive upright emissions with no reflection give  $R_{\text{no reflection}} \rightarrow \infty$ .  $R$  as a function of atmospheric optical thickness is summarized in Table 3.

**Table 3.** The ratio of zenith brightness to horizontal illuminance as a function of atmospheric optical thickness  $\tau_0$  for an exponentially stratified atmosphere.

Model	$F$	$G$	$\tau_0$	$\eta$	$\rho$	$R$
Garstang's model	0.15	0.15	0.0	1.0	0.35	$\pi/0.48$
			0.2	0.567	0.107	$\pi/0.69$
			0.5	0.258	0.032	$\pi/0.85$
			1.0	0.075	0.0052	$\pi/0.97$
no uplight	0.0	any	0.0	1.0	0.35	$\pi \approx 3.14$
			0.2	0.567	0.107	$\pi/1.14$
			0.5	0.26	0.032	$\pi/1.28$
			1.0	0.075	0.0054	$\pi/1.40$
dirty snow cover	0.15	0.45	0.0	1.0	0.35	$\pi/0.74$
			0.2	0.567	0.107	$\pi/0.94$
			0.5	0.258	0.032	$\pi/1.09$
			1.0	0.075	0.0052	$\pi/1.22$
snow cover (model 3)	0.15	0.75	0.0	1.0	0.35	$\pi/0.82$
			0.2	0.567	0.107	$\pi/1.01$
			0.5	0.258	0.032	$\pi/1.16$
			1.0	0.075	0.0052	$\pi/1.29$

The limiting value of  $R$  for extremely low values of  $\tau_0$  is  $\pi$  (no uplight). However,  $\lim_{\tau_0 \rightarrow 0} B(z) = 0$ , so  $D = \pi B(0) \equiv 0$ . In a slightly polluted atmosphere (i.e. at low values of  $\tau$ ),  $D/B(0)$  can be as high as  $\approx 2\pi$  for Garstang-like cities with  $F = G = 0.15$ . The corresponding value for the model of a homogeneous atmosphere is almost 2 times smaller (consult Table 2). It is caused by a more rapid intensity decay if beams propagate at low elevation angles in a homogeneous atmosphere. Since the concentration of atmospheric constituents in a homogeneous atmosphere is not a decreasing function of altitude, this kind of model has tendency to generate more efficient attenuation of light beams than in the case of an exponentially stratified atmosphere. However, values of  $R$  can change with optical thickness. Large optical thickness implies large attenuation, but also more intensive scattering. It is well known that both of these processes show opposed effects. The diffuse light of a night sky benefits from elevated scattering efficiency, but at the same time it suffers from enhanced attenuation. Such a functional dependence can be written very roughly in form  $\sim \tau_0 e^{-c\tau_0}$  (compare with the exact equation 8). The attenuation of light beams would dominate in an atmosphere with  $\tau_0$  above a peak value (such as  $1/c$ ). If  $\tau_0$  is below this limit value, scattering would play a pivotal role, especially for low zenith angles.

## 2.5 Ratios of horizontal illuminance to zenith brightness other than $\pi$

The  $F$  or  $G$  values are rarely below 0.1. The theoretical models introduced above most typically suggest that  $R \approx \pi$ . However, values of  $\approx \pi$  usually represent a lower limit for the ratio of horizontal illuminance to zenith brightness, because it was obtained under the assumption of pure backscatter. An optical device situated in a realistic finite-sized city records the light signals scattered in all directions, mostly backwards and sideways (see fig. 1 in Kocifaj 2014). The number of photons produced by sidescatter is usually several times larger than the corresponding amount of photons emitted backwards. The larger the distance from a city, the higher the importance of side scatter (or alternatively forward scatter). In any case, the value of  $D$  in a realistic finite-sized city would be larger than that computed from the previous formulae. Therefore the observed data would suggest  $R > \pi$ , corresponding to a sky brightness increasing with zenith distance (see below). By contrast, some of the cases with  $R < \pi$  in our models correspond to situations where the sky is brighter close to the zenith than near the horizon (e.g. for some models with snow).

Assuming a hypothetical observer is situated in the centre of a large, nearly circular city, the brightness becomes a monotonically increasing function of the zenith angle. Such a behaviour is independent of the azimuth angle and the function can be roughly approximated by  $\sec(z) = 1/\cos(z)$ . Such a zenith distance dependence of the sky brightness is also supported by recent measurements performed in the Vienna–Bratislava region during clear nights. Replacing  $B(\phi, z)$  in equation (2) with  $1/\cos(z)$ , we obtain

$$D = B_0 \int_{\phi=0}^{\phi=2\pi} d\phi \int_{z=0}^{z=\pi/2} \sin z dz, \quad (21)$$

which yields

$$D = 2\pi B_0, \quad (22)$$

so the ratio  $R$  can become as large as  $2\pi$ . This value is roughly consistent with more accurate simulations made for Garstang’s light sources (see figs 5–7 in Kocifaj 2011, where the values  $\sim 1/R$  are plotted).

## 3 APPLICATIONS TO DATA MEASURED AT THE VIENNA UNIVERSITY OBSERVATORY

Since 2011 November, we have been measuring the zenith night sky brightness at the Vienna University Observatory, which is located 3 km to the north-west of Vienna’s city centre. We use the already mentioned SQM, equipped with an ethernet connection, for our measurements. For every night with a sufficient amount of data, the average zenith night sky brightness (NSB) in magnitudes per square arcsec is calculated. As reported in a previous article (Puschnig et al. 2014), the best (= darkest) night-averaged NSB values at this site reach  $\sim 19.3 \text{ mag}_{\text{SQM}} \text{ arcsec}^{-2}$ . The circalunar modulation of the average NSB is difficult to see in the data recorded at the Vienna University Observatory, since the presence or absence of clouds is by far the dominant effect at this site. Note that cloud arrays act as strong enhancers of the artificial NSB.

In the present section, we will show an application of the results presented in the theoretical sections of this article to the above-mentioned measurements. Fig. 2 shows the night-averaged NSBs derived in Vienna with SQM measurements between 2011 November and 2014 July. The mean NSBs vary over almost five magnitudes, corresponding to a factor close to 100 in intensity. However, skies brighter than  $15.5 \text{ mag}_{\text{SQM}} \text{ arcsec}^{-2}$  only occur during winter nights with snow, which strongly enhances the reflectivity of the ground, in combination with clouds enhancing the backscattering by the atmosphere. (This is consistent with the darker winter nights between 2013 December and 2014 February, since that particular winter was mild and snow-poor at our observing site). On the other hand, the three summer periods included in Fig. 1 (2012/2013/2014) are clearly characterized by darker mean NSB values. This is due not only to the absence of snow but also to the lantern-shielding effect of trees and other types of vegetation.

The effect of snow cover on  $R$  can be simulated using equation (19), while the computational results are summarized in Table 3. Garstang-like values of  $R$  are lowered by approximately 25–35 per cent under dirty snow conditions (or 35–40 per cent in the case of fresh snow). This implies that snow-free surfaces cause a steeper increase of sky brightness from the zenith towards the horizon. In other words, the snow-cover smooths luminance patterns, resulting in  $R_{\text{snow}} < R_{\text{snow-free}}$ .

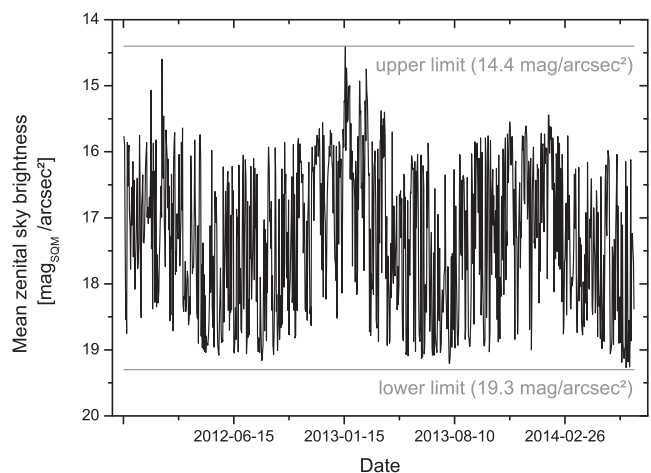


**Figure 2.** Night-averaged zenith sky brightness measured at Vienna University observatory from 2011 November–2014 July using an SQM.

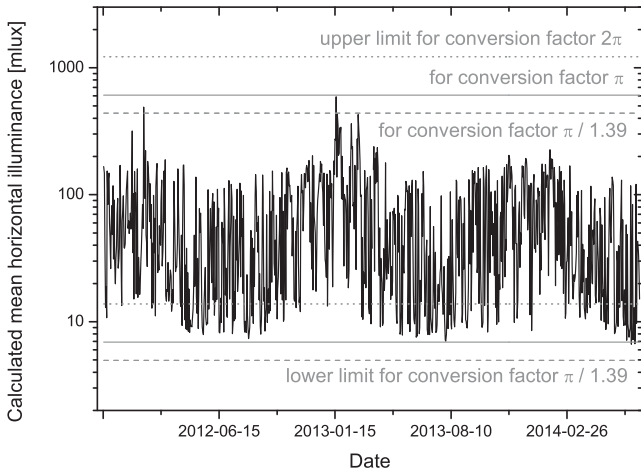


**Figure 3.** Horizontal diffuse illuminances computed using experimental data depicted in Fig. 2. See text for details.

From the NSBs measured in  $\text{mag}_{\text{SQM}} \text{ arcsec}^{-2}$ , we deduce the zenith luminance [ $\text{cd m}^{-2}$ ] by the empirical relation (e.g. Garstang 1986, equation 19)

$$\text{Luminance} = 10.9 \times 10^4 \times 10^{(-0.4 \times [\text{mag arcsec}^{-2}])}. \quad (23)$$

In application to the mean NSBs shown in Fig. 2, this leads to a range of night-averaged zenith luminances between 2.1 and 190  $\text{mcd m}^{-2}$ , which is between 10 and 950 times the natural zenith sky luminance.

We now turn back to the question of horizontal illuminance. Ideally, the conversion between mean zenith luminance and mean horizontal illuminance should be done with a different conversion factor for each individual night, since the distribution of luminance over the night sky varies significantly with optical depth, reflectivity of the ground, etc. However, a detailed, time-dependent conversion is not possible on the basis of the available data. Therefore, we focus on the implications of the previous theoretical calculations for the *order of magnitude* of the horizontal illuminance.

It has been demonstrated in Section 2 that, for most realistic models of light propagation in the atmosphere, the conversion factor  $R$ , defined as the ratio of horizontal illuminance to zenith brightness, is between  $\sim 2.26(\pi/1.39)$  and  $2\pi$  (Section 2.3–2.5). Fig. 3 illustrates what this means in terms of (realistic) upper limits to the horizontal illuminance. While the canonical value  $R = \pi$  implies – for our measurement site – a range of night-averaged horizontal illuminances between 6.9 and 609  $\text{mlux}$ , we now infer, from the range of realistic  $R$  values derived in Section 2, an illuminance range of up to 1.2 lux (see upper dotted line in Fig. 3).

Since night sky brightnesses are measured on a continual basis at the University of Vienna, further improvements of our model are possible after processing long-term data sets.

#### 4 CONCLUDING REMARKS

The diffuse horizontal illuminance  $D$  is the cosine-projected brightness  $B$  integrated over the whole sky vault, thus being a satisfactorily representative quantity for the characterization of the overall optical state of the night sky. The illuminance is traditionally measured by luxmeters, for which in many cases the dynamic range is, however, not large enough for monitoring the night sky brightness, especially in natural spaces or near small towns. Instead, SQMs are preferred, since these instruments are designed to operate under low illumi-

nation levels. SQMs record near-zenith brightness  $\simeq B(0)$ , which is difficult to interpret in terms of total downwelling luminous flux. In general, the mapping from  $B(0)$  to  $D$  is scarcely possible without a well-founded theoretical model. However, such a transformation is strongly needed because a vast data base of  $B(0)$  already exists for many places in the world, while  $D$  is measured infrequently.

In the present article, we have developed approximations in order to convert zenith luminance measurements into horizontal diffuse illuminance levels. The simplest model is based on a two-stream approximation assuming a uniformly emitting surface. The ratio of  $D$  to  $B(0)$  is obtained as a correction factor to the canonical value of  $\pi$  for uniform sky brightness. While the two-stream approximation typically leads to a factor  $>1$ , the model of a homogeneous attenuating atmosphere illuminated by a finite-sized light source instead suggests a factor below 1.0, i.e.  $D = \text{factor} \times \pi$ . The most appropriate approximation is developed as an analytical extension to the model of an exponentially stratified atmosphere with varying optical depth  $\tau$ . Assuming Garstang-like light sources with uplight fraction  $F \approx 0.15$  and portion of reflected light  $G \approx F$ , the computed ratios are found to be  $R \gtrsim \pi$  for an optically thin atmosphere. However, snow cover can change the situation, due to efficient reflection from ground surfaces that makes  $R \lesssim \pi$ . The same is observed for extremely low values of  $F$ .

An application of our theoretical formulae was demonstrated by deriving lower and upper limits to the horizontal illuminance from data sets of zenith luminance data collected at the Vienna University Observatory. The model we have developed is designed for routine use in processing SQM data at any site accepting territory-specific values of  $F$  and  $G$  as well as the optical thickness of an atmospheric environment. Further improvements are possible, but wider statistics is required to identify the model that best fits the experimental data. Field campaigns usually do not include information on clouds, therefore the present solution concepts represent a trade-off between exact models and empirical approaches.

#### ACKNOWLEDGEMENTS

This work was supported by the SAIA in the Framework of Action Austria–Slovakia (Co-operation in Science and Education), by the Slovak Research and Development Agency under contract No. APVV-0177-10 and by the Slovak National Grant Agency VEGA (grant No. 2/0002/12). HASL received a support from the National Council of Science and Technology of Mexico, under the project Cátedras CONACYT # 2723 TP, and MK furthermore acknowledges travel grants from the EU-COST project ES 1204, ‘Loss of the Night Network’. We thank Andrej Mohar (Ljubljana) for providing results of his all-sky measurements performed between Vienna and Bratislava.

#### REFERENCES

- Aubé M., Kocifaj M., 2012, MNRAS, 422, 819
- Bennie J., Davies T. W., Duffy J. P., Inger R., Gaston K. J., 2014, Contrasting trends in light pollution across Europe based on satellite observed night time lights. Scientific Reports, 4, 3789
- Biggs J. D., Fouché T., Bilki F., Zadnik M. G., 2012, MNRAS, 421, 1450
- Cinzano P., 2000a, Mem. Soc. Astron. It., 71, 93
- Cinzano P., 2000b, Mem. Soc. Astron. It., 71, 159
- Cinzano P., 2005, Night sky photometry with sky quality meter. ISTIL Int. Rep. Istituto di Scienza e Tecnologia dell’Inquinamento Luminoso, Thiene, Italy, 9
- Cinzano P., Falchi F., 2003, Mem. Soc. Astron. It., 74, 458
- Cinzano P., Falchi F., 2012, MNRAS, 427, 3337

- Cinzano P., Falchi F., Elvidge C. D., 2001, *MNRAS*, 328, 689
- Duriscoe D. M., Luginbuhl C. B., Moore C. A., 2007, *PASP*, 119, 192
- Falchi F., 1999, Masters thesis, Milan Univ.
- Falchi F., 2011, *MNRAS*, 412, 33
- Garstang R. H., 1986, *PASP*, 98, 364
- Garstang R. H., 1989a, *PASP*, 101, 306
- Garstang R. H., 1989b, *BAAS*, 21, 759
- Garstang R. H., 1991, *PASP*, 1109
- Geffen K. G., Grunsven R. H., Ruijven J., Berendse F., Veenendaal E. M., 2014, *Ecology and Evolution*. Vol. 4, p. 2082
- Guo D. F., Hu S. M., Chen X., Gao D. Y., Du J. J., 2014, *PASP*, 126, 496
- Kocifaj M., 2007, *Appl. Opt.*, 46, 3013
- Kocifaj M., 2011, *MNRAS*, 415, 3609
- Kocifaj M., 2014, *J. Quant. Spectrosc. Radiative Transfer*, 139, 43
- Kocifaj M., Solano Lamphar H. A., 2014, *MNRAS*, 439, 3405
- Kolláth Z., 2010, Measuring and modelling light pollution at the Zselic Starry Sky Park, in *Journal of Physics: Conference Series*, Vol. 218, No. 1. IOP Publishing, p. 012001
- Kyba C. C., Ruhtz T., Fischer J., Hölker F., 2011, Cloud coverage acts as an amplifier for ecological light pollution in urban ecosystems. *PLoS one*, 6(3), e17307
- Kyba C. C. M. et al., 2013, *Sci. Rep.*, 3, 1835
- Luginbuhl C. B., Boley P. A., Davis D. R., 2014, *J. Quant. Spectrosc. Radiative Transfer*, 139, 21
- McCartney E. J., 1977, *Optics of the Atmosphere*. John Wiley & Sons, Chichester
- Müller A., Wuchterl G., Sarazin G., 2011, *Rev. Mex. Astron. Astrofiz. Conf. Ser.*, 41, 46
- Perry G., Buchanan B. W., Fisher R. N., Salmon M., Wise S. E., 2008, in Mitchell J. C., Jung Brown R. E., Bartholomew B., eds, *Herpetological Conservation*. Society for the Study of Amphibians and Reptiles, Salt Lake City, UT, p. 239
- Pun C. S. J., So C. W., 2012, *Environmental Monitoring and Assessment*, 184, 2537
- Puschig J., Posch Th., Uttenthaler S., 2014, *J. Quant. Spectrosc. Radiative Transfer*, 139, 64
- Rich C., Longcore T., 2005, *Ecological consequences of artificial night lighting*. Island Press, Washington, D.C
- Riddle R. L., Walker D., Schöck M., Els S. G., Skidmore W., Travouillon T., Gregory B., 2008, An analysis of light pollution at the Thirty Metre Telescope candidate sites. In *SPIE Astronomical Telescopes+ Instrumentation*. International Society for Optics and Photonics, p. 701223
- Solano Lamphar H. A., Kundracik F., 2014, *Lighting Research and Technology*, 46, 20
- Wise S., 2007, in Marin C., Jafari J., eds, *Proc. StarLight: a Common Heritage*. La Palma, April 19-20, p. 107

This paper has been typeset from a  $\text{\TeX}/\text{\LaTeX}$  file prepared by the author.